Arch. Mech., **51**, 6, pp. 717–726, Warszawa, 1999

Experimental investigations of thermomechanical couplings in TiNi shape memory alloy during a torsion-tension (compression) test

W. OLIFERUK

Polish Academy of Sciences
Institute of Fundamental Technological Research,
Świętokrzyska 21, 00–049 Warsaw, Poland
e-mail: wolif@ippt.gov.pl

EXPERIMENTAL INVESTIGATIONS of thermomechanical coupling in TiNi alloy during uniaxial and biaxial loading at the temperature higher than the room temperature is presented. The applied method is based on contactless temperature measurements. The results of the investigations are reported. They are interpreted in terms of the phase transitions.

1. Introduction

THE SHAPE-MEMORY EFFECT (SME) in the TiNi alloy appears as a result of phase transitions. The kind of phase transitions depends on the range of mechanical and thermal loading of the material tested. During phase transitions, the thermomechanical couplings take place. Some part of the expended mechanical energy is dissipated in the form of heat (exoenergic process). Because of this, temperature of the tested sample increases. When the phase transitions process is endoenergic, the temperature of the sample decreases.

The measurements of temperature changes of the sample due to thermomechanical coupling are important for understanding the overall deformation behaviour of shape-memory alloys (SMA) and they give a basis for verification of the constitutive thermomechanical models describing this behaviour. Such statement results first of all from high temperature sensitivity of most of the SMA.

The present work is devoted to experimental investigations of the thermomechanical coupling in TiNi sample during the uniaxial and biaxial loading at a low level of stress range, where the B2 $\leftrightarrow$ R transition proceeds.

The temperature measurements of the sample of TiNi alloy were carried out during: (1) – *torsion*, (2) – *tension*, (3) – *compression*, (4) – *simultaneous torsion*

(shear stress τ) and *tension* (axial stress σ) ($m = \tau/\sigma = 1$) and (5) - *torsion-compression* ($m = -1$) tests, at different temperature ranges. The tests were performed on a tubular sample. It was strained (to a limited extent) on an Instron testing machine with constant stress rate equal to 1 MPa/s. The details of the test program and the conditions of experiments are given in the papers [1, 3]. First part of this program includes the investigations of five various loading paths at a low temperature range: 200 K, 280 K, 300 K and the maximum effective stress equal to 100 MPa, when reorientation of the pre-existing R-phase occurs; in other words, when the strain is the result of a twinning process. If the ambient temperature is different than the room temperature, the use of a temperature chamber is required. The temperature was measured on the basis of detection of IR radiation of the sample under test. It has been found that the change of sample temperature during the twinning process is negligible (is not higher than 1K). At the chamber temperature lower than the room temperature, higher accuracy was impossible because of the temperature instability of the chamber used.

There exist many works on contactless sample temperature measurements during deformation tests of metals carried out at the room temperature, without the use of a temperature chamber. However, as far as the author is aware, there exists no work on contactless monitoring of the temperature sample during multiaxial loading tests carried out in a temperature chamber.

Detection of IR radiation was applied to determine the heat of the Austenite-Martensite (A $\leftrightarrow$ M) phase transition in Cu Zn Al SMA in [2].

In the present paper, the results of the instantaneous temperature measurements of the TiNi alloy sample during uni- and multiaxial loading at 310 K and in the range of stresses, where B2 $\leftrightarrow$ R phase transitions take place, are given. The maximum of effective stress was equal to 290 MPa. In such conditions, the temperature stability of the chamber used was better than at the temperature lower than the room temperature.

2. Temperature measurements based on infrared radiation detection

The contactless temperature measurements are based on the Stefan Boltzmann formula stating that the total power M_{bb} of infrared radiation (IR) emitted by a black body is a single-valued function of its temperature T.

$$M_{bb} = \xi \cdot T^4, \tag{2.1}$$

where ξ is the Stefan Boltzmann constant, $\xi = 5.7 \cdot 10^{-8} \mathrm{Wm^{-2}K^{-4}}$. Thus, by measuring the IR radiation power emitted by the tested object, it is possible to determine its temperature. Such a measurement does not disturb the temperature field of the object.

However, the real object behaviour never complies with the Eq. (2.1).

The factor required to describe the IR radiation produced by a real object is called emissivity. The spectral emissivity ε_λ is defined as the ratio of spectral radiant emittance from an object to that emitted from a black body at the same temperature and wavelength.

The Stefan Boltzmann formula for real objects takes the form:

$$M = \varepsilon \cdot \xi \cdot T^4, \tag{2.2}$$

where ε is the average emissivity within the range from $\lambda = 0$ to $\lambda = \infty$.

According to Kirchhoff's law, for any material, the spectral emissivity is equal to the spectral absorbance of an object at any specified temperature and wavelength. When the object is non-transparent, the formula for the complex IR detector response signal S can be written as:

$$S = \varepsilon \cdot f(T_0) + (1 - \varepsilon) \cdot f(T_i), \tag{2.3}$$

where T is the object temperature, T_i is the ambient temperature, $\varepsilon f(T_0)$ – signal as a function of the object temperature, $(1-\varepsilon)f(T_i)$ – signal as a function of the ambient temperature.

In order to determine the non-transparent object temperature, the emissivity of this object, the ambient temperature and function $f(T)$ which is the calibration curve of an IR detector or the whole measurement instrument must be known.

In the experiments described hereafter, the temperature of the sample surface was determined using the Infrared Camera of the 680 type, manufactured by the AGA Company. It is equipped with the indium antimonide (InSb) IR detector. The response time of this detector is shorter than one microsecond. Its response sets in (2.5 – 5.5) μm range of wavelength.

The Infrared Camera principle of operation is as follows: an optical-mechanical scanner scans the tested surface and focuses the IR radiation on the InSb detector, which converts the IR signal into an electrical video one. The scanner gives the thermal image of the tested surface.

Operation of the Infrared Camera is modified by application of the PTR WIN System manufactured by the CEDIP Company. The PTR WIN consists of the digitiser and the PTR software. It allows to digitise the video signal into 12 bits digital one with sampling frequency of 1 MHz.

The thermal image is displayed on a computer screen. The PTR WIN System allows for digitising and then continuous storing of the film of IR images in the hard disc(16 frames per second). The PTR 9020 software allows for the digital processing of thermal images, for example: the temperature measurement along an arbitrarily selected line of the tested surface.

3. Experiments

The investigations of the thermomechanical couplings in the TiNi alloy during loading at temperature 310 K require the use of the temperature chamber. The contactless measurement of the sample temperature requires a window in the chamber, which is transparent for IR radiation in the (2.5 – 5) μm spectral range. The single crystal of silicon has got such a property.

The old chamber-equipment of the testing machine was adopted. There the glass window was replaced by a silicon one. The IR transmission of the silicon window in the (3 – 5) μm spectral range reaches 85%. Owing to this window, the IR radiation power emitted by the sample could be measured as a function of the deformation process parameters. The surface area, where the IR radiation power was measured, was blackened to ensure a homogeneous and known emissivity of the surface.

The calibration curve for Infrared Camera with silicon chamber window was obtained.

The experiment was performed on the thin-walled tube made of TiNi alloy (Fig. 1).

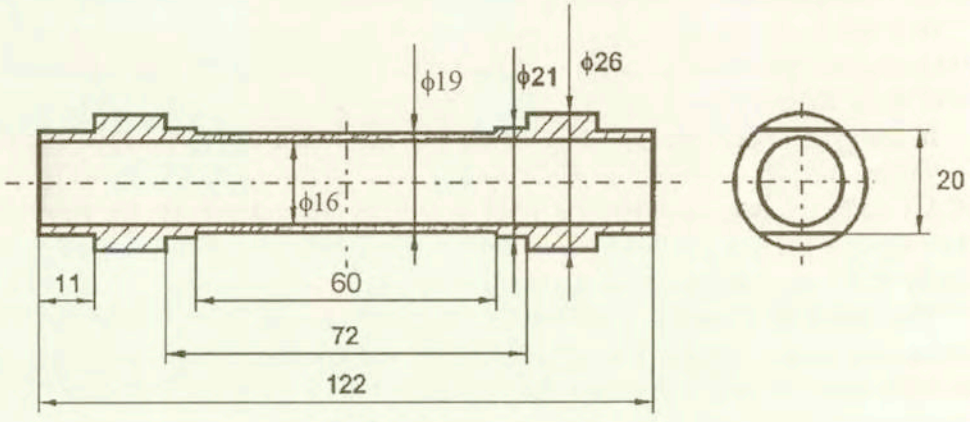

FIG. 1. The shape of the tested sample.

The temperature of the sample as function of effective stress during (1) – *torsion*, (2) – *tension*, (3) – *compression*, (4) – *simultaneous torsion* (shear stress) and *tension* (axial stress σ) ($m = \tau/\sigma = 1$) and (5) – *torsion – compression* ($m-1$) test at the chamber temperature 310 K was measured.

All tests have been carried out on the multiaxial Instron testing machine equipped with the MTS Test Star fully digital controller connected to the computer [3]. The sample was heated up to 343 K after each loading in order to recover the initial state of microstructure.

4. Results

Because of the cylindrical shape of the sample, only the temperature distribution along a generating line of the tested sample has been determined. Figure 2 shows the examples of the temperature distribution on the blackened area of the sample surface at $\sigma_0 = 0$ (Fig. 2a) and during the tension at $\sigma_2 = 198$ MPa (Fig. 2b), $\sigma_3 = 281$ MPa, at which the temperature increase was the highest (Fig. 2c). Fig. 3 shows the increase of the temperature as the difference between the temperature along the generating line at $\sigma = 198$ and $\sigma = 0$ MPa.

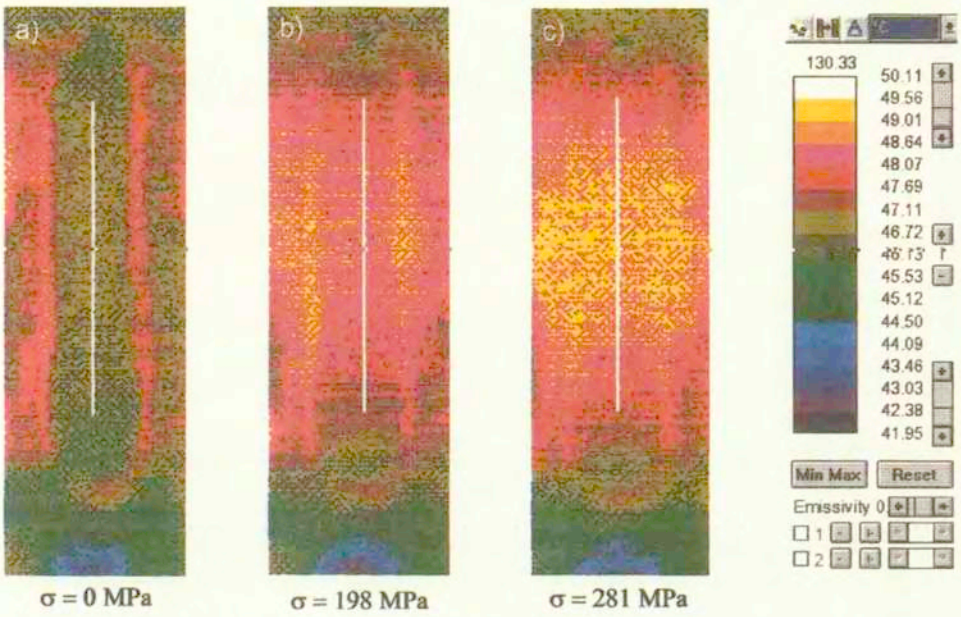

FIG. 2. Examples of thermal images of the sample during the tensile test of the TiNi shape memory alloy under constant stress rate = 1MPa/s.

It was observed that the temperature distribution along the generating line of the sample was approximately uniform. The temperature distributions along the generating line of the sample during other tested deformation paths were also uniform. It indicates that phase transition processes in the tested sample were almost homogeneous.

With the aid of Infrared Camera, the monitoring of the chamber temperature during loading and unloading was possible. The results of such monitoring are presented in Fig. 4. The chamber temperature variation (ΔT_{ch}) was about 0.2 K.

The strain-stress curves of TiNi shape memory alloy for five proportional stress-controlled loading paths are shown in Fig. 5. They exhibit clearly the pseudoelastic effect associated with the B2 $\leftrightarrow$ R transition. The area limited by

the strain-stress curve is close to the expended energy in the loading-unloading cycle. Figure 5 shows that this energy depends on the loading path. It is the highest during tension (Fig. 5, curve 2) and the lowest one during compression (curve 3). This fact can not be explained by the tested alloy anisotropy alone, because the third invariant of stresses in an individual loading path is not the same.

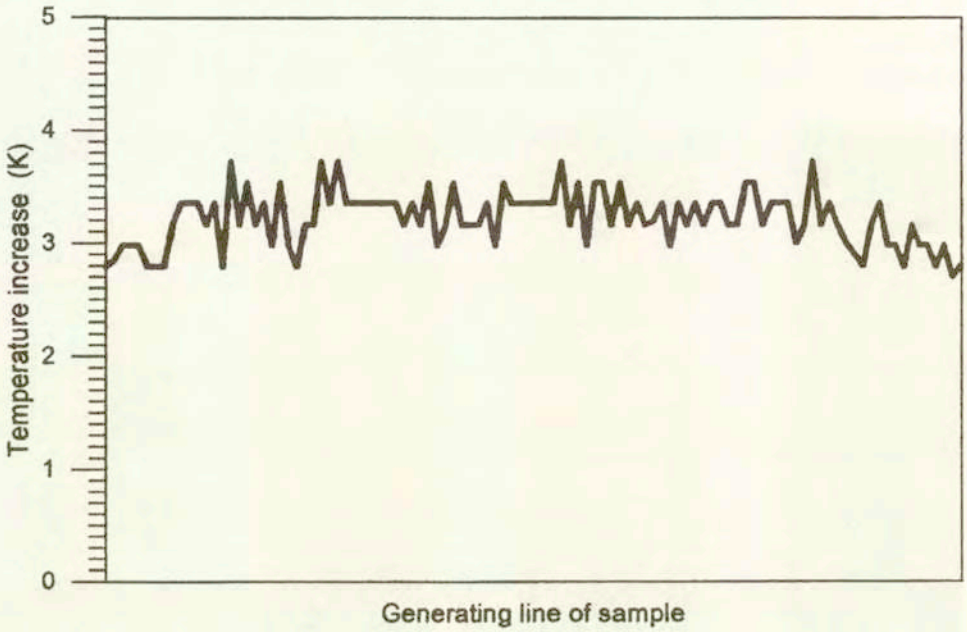

FIG. 3. The temperature increase distribution along the generating line of the sample of TiNi alloy at $\sigma = 198$ MPa during the tensile test at the chamber temperature of 310 K.

The expended energy is equal to the heat dissipated by the tested sample, provided that the state of the sample after unloading is recovered. However, the area limited by the strain-stress curve may, in general, be not equal to the total work done in the cycle [4].

The dissipated energy and the heat of phase transition generate variations of the sample temperature. It can be expected that when the hysteresis loop (shown in Fig. 5) is thicker, the maximal increase of sample temperature in the cycle is higher.

Thus, on the basis of the results presented in Fig 5 it can be expected that the temperature increase should be the greatest one in tension and the smallest one in compression.

The changes of average temperature along the generating line as the function of the effective stress are presented in Fig. 6 ($\sigma_{ef} = \sqrt{\sigma^2 + 3\tau^2}$, see reference [4]). The maximum of effective stress was equal to 290 MPa. In such a case only the

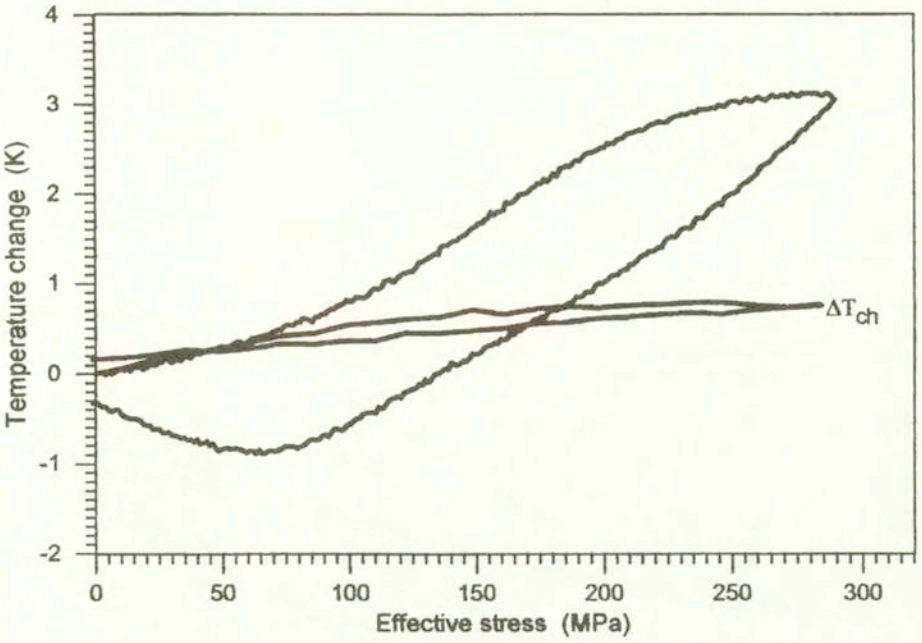

FIG. 4. The temperature change of the TiNi sample during tension and the chamber temperature variation (ΔT_{ch}) due to the temperature instability of the chamber used.

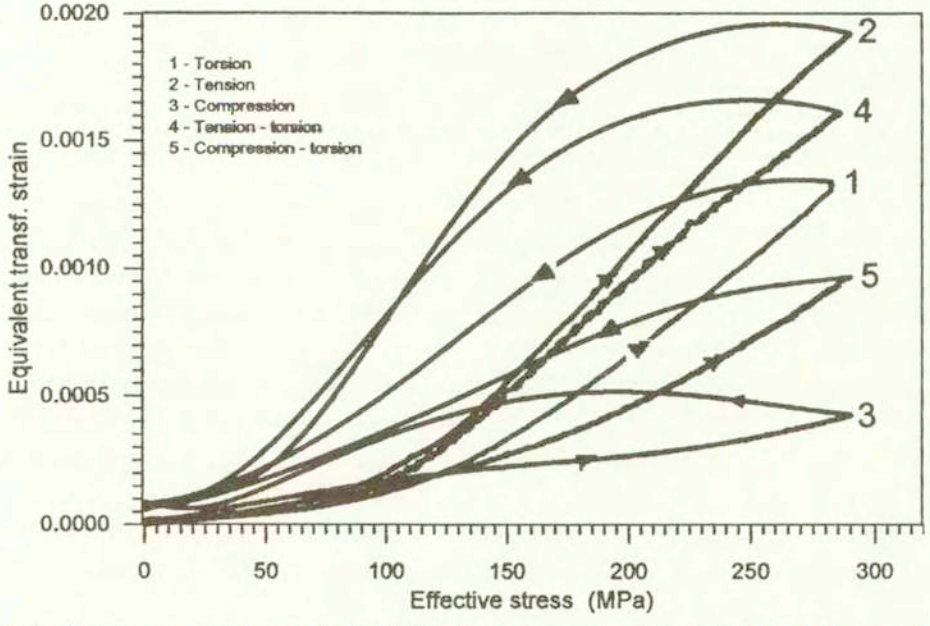

FIG. 5. Strain-stress curves of the TiNi shape memory alloy loaded at the constant stress rate = 1 MPa/s at 310 K.

B2 ↔ R phase transition is possible. The expectation has been confirmed by all the tested loading paths except the compression (Fig. 6, curve 3), where the increase of sample temperature is not the smallest one.

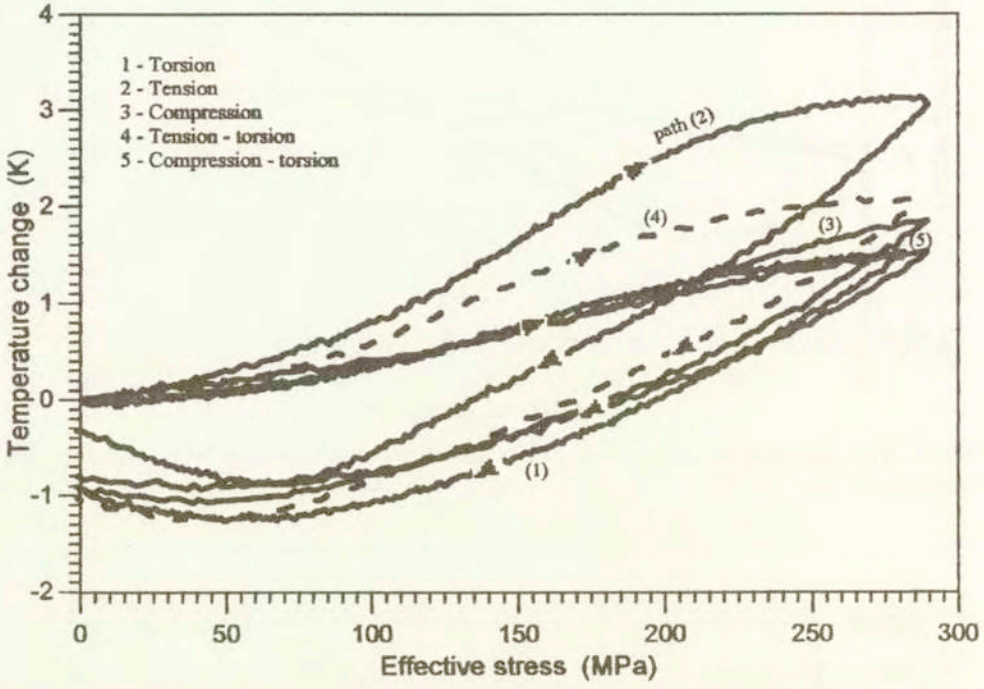

FIG. 6. The change of sample temperature vs. the effective stress during loading at constant stress rate = 1 MPa/s at 310 K.

It is known that the B2 ↔ R phase transition is exoenergic. The existence of the hysteresis loops proves that the process of deformation is dissipative. These effects cause the observed increase of the sample temperature in the course of loading. During unloading, the reverse transition R ↔ B2 takes place and the temperature of the sample decreases. It attains the value below the temperature of the chamber. Some energy was taken by the sample. We can observe that in the last stadium of unloading, the temperature of the sample started to rise (Fig. 6, curves 1, 2). This is related to the pure elastic behaviour of the investigated alloy. The sample is warmed by the environment.

The observed temperature variations suggest that progress of the B2 ↔ R phase transitions was most advanced in the tension test while the least advanced progress was observed during a pure shear (*torsion*) test.

The temperature changes of the tested sample during loading are shown in Fig. 7. It is observed that the reverse R ↔ B2 phase transitions in all of the tested loading paths proceed more rapidly than the B2 ↔ R phase transitions.

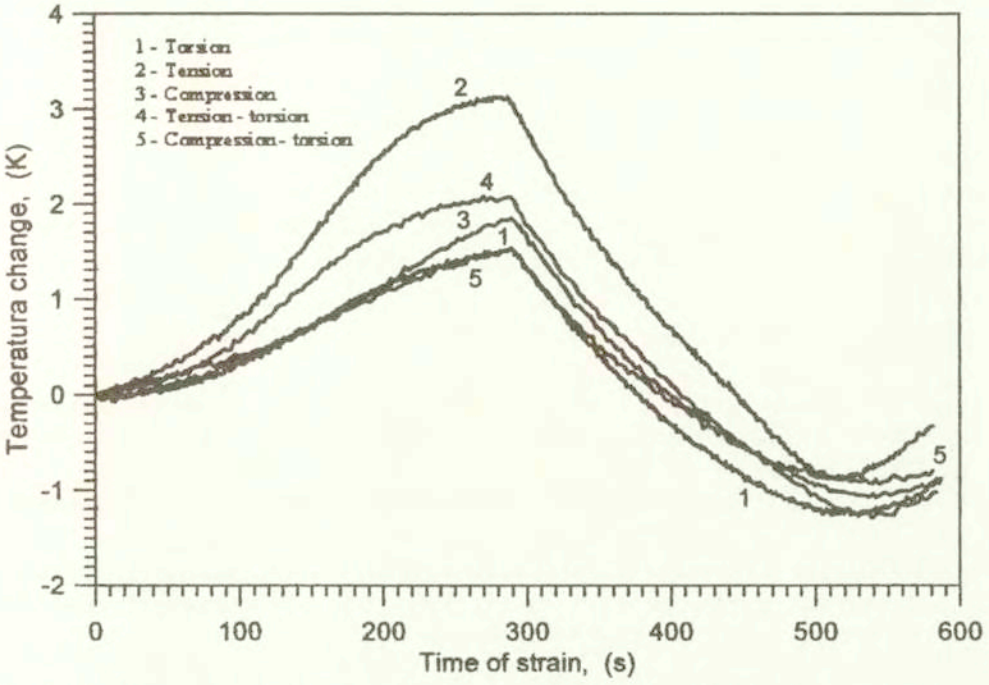

FIG. 7. The temperature change of the tested sample during the loading cycles for five proportional loading paths.

5. Some remarks concerning the results

The detection of IR radiation has been successfully applied to investigate the thermocouplings in the TiNi alloy during loading at temperatures higher than the room temperature.

It has been observed that the temperature distribution along the generating line of the sample during five different loading tests performed at constant rates is approximately uniform. It indicates that phase transition processes in the tested sample are homogeneous.

The energy expended during the loading-unloading cycle depends on the deformation path.

The temperature change of the sample under test ($\sigma_{ef\,\max} = 290$ MPa) shows that kinetics of the B2 $\leftrightarrow$ R phase transitions and the reverse ones are different; the R $\leftrightarrow$ B2 phase transitions proceeds more rapidly. It concerns all the tested deformation paths.

It has been found that progress of the B2 $\leftrightarrow$ R phase transitions was most advanced in tension while the least advanced progress is observed during the pure shear (*torsion*) and during the *compression-torsion* test ($\sigma_{ef\,\max} = 290$ MPa).

The effect of the deformation path on the expended energy is in accordance with the temperature change of the sample during the particular loading path, except the case of compression.

Acknowledgements

This work has been supported by State Committee for Scientific Research (Poland) under Grants No. 7T 07A 00513 and 7T 08A 025 11.

References

1. B. RANIECKI, S. MIYAZAKI, L. DIETRICH, K. TANAKA and CH. LEXCELLENT, *Deformation behaviour of TiNi SMA undergoing phase transition in torsion – tension (compression) tests*, Arch. Mech, (in print) 1999.
2. CH. LEXCELLENT, G. ROGUEDA, C. BOURBON, *Continuum Mech. and Thermodynamics*, **6**, 4, 1994.
3. B. RANIECKI, L. DIETRICH, Z. KOWALEWSKI, G. SOCHA, S. MIYAZAKI and A. ZIÓŁKOWSKI, *On experimental techniques used to investigate deformation behaviour of TiNi under complex stress state*, Arch. Mech, (in print) 1999.
4. B. RANIECKI, CH. LEXCELLENT, Eur. J. Mech., A/Solids, **13**, 1, 21–50, 1994.

Received April 28, 1999; revised version November 11, 1999.